J. Basic. Appl. Sci. Res., 2(4)3926-3934, 2012

ISSN 2090-4304
Journal of Basic and Applied Scientific Research
www.textroad.com

Numerical Simulation of Axial Compressor Rotor Flow Using Two Dimensional Euler Equations

S.Niazi, Y.Bakhshan and M.Pourreza

Department of Mechanical Engineering, Hormozgan University, Bandar Abbas, Hormozgan, Iran

ABSTRACT

Numerical simulation of two dimensional inviscidflow through axial compressor rotor blades is presented. Appropriate partial differential equations have been solved numerically to generate an orthogonal H-type grid which is clustered densely near regions of high gradients. The set of conservation equations of mass, momentum and energy were solved assuming inviscid and compressible real gas flow and the movement of rotor blades was taken into account using Arbitrary LagrangianEulerian formulation. A finite volume approach was employed which is based on a flux difference splitting scheme for the calculation of face fluxes and takes advantage of artificial viscosity terms to damp the spatial oscillations near shocks. An entropy correction has been included to prevent any unphysical expansion shock to form. The used method was validated against a number of test cases including Sod shock tube problem, converging diverging nozzle and flow over a bump inside a channel. The simulations for achieving the final results were carried out for a compressor rotor named NASA Rotor35 and the results were compared with the available experimental data. It is concluded that solving Euler equations on the midspan of the rotor can give an assessment of total pressure and temperature rise of the rotor.

INTRODUCTION

Axial compressors are widely used in different industry branches due to their unique specifications like large flow capacity and high efficiency. The performance of these turbomachinesrelies heavily on the performance of their moving parts, i.e. their rotors which transfer the received energy from the external source to the fluid being compressed. In the present work, CFD analysis of axial compressor rotor is presented. The flow is mainly assumed to be two dimensional and the geometry consists of a midspan section of the rotor in which, the blades are seen as a cascade of moving airfoils. Flow through two successive blades is of interest because of the rotor symmetry and high amounts of computations needed to simulate a complete rotor.Also, the flow is considered to be inviscid and hence, the governing equations and the set of boundary conditions used correspond to a flow with no effect of viscosity.

As the finite volume approach is used for the spatial discretization of the governing equations, the calculation of fluxes through faces of computational cells becomes a very important part of the numerical method. Several methods have been proposed for the calculation of inviscid fluxes which vary in capabilities and computational costs. In the present study, Roe's method [1] has been used as the flux evaluation scheme, and the artificial viscosity terms of the method have been replaced by a generalization of these terms proposed by Liu et al. [2] for its lower amounts of computations needed. Generally, Roe's method has a need of a so called "entropy correction" or "entropy fix" to prevent unphysical expansion shocks in the solution. The correction proposed by Phongthanapanich et al. [3] has been used in this study to perfect the numerical method for which details will be explained in the following sections.

GOVERNING EQUATIONS

The governing equations are those of inviscid and compressible ideal gas flows which are usually called the system of Euler equations. Using ALE formulation to consider the movement of the rotor, the set of the governing equations in flux vector form will be: [4]

***Corresponding Author:** Y.Bakhshan, Department of Mechanical Engineering, Hormozgan University, Bandar Abbas, Hormozgan, Iran.

$$\frac{\partial Q}{\partial t}+\frac{\partial F}{\partial x}+\frac{\partial G}{\partial y}=0 \quad (1)$$

Where

$$Q=\begin{bmatrix}\rho\\ \rho u\\ \rho v\\ \rho E\end{bmatrix}\ F=\begin{bmatrix}\rho(u-u_g)\\ \rho u(u-u_g)+p\\ \rho(u-u_g)v\\ \rho E(u-u_g)+pu\end{bmatrix}\ G=\begin{bmatrix}\rho(v-v_g)\\ \rho u(v-v_g)\\ \rho v(v-v_g)+p\\ \rho E(v-v_g)+pv\end{bmatrix} \quad (2)$$

$$p=(\gamma-1)\rho\left[E-\frac{u^2+v^2}{2}\right] \quad E=c_vT+\frac{u^2+v^2}{2} \quad (3)$$

Here, u_g and v_g are velocity components of the computational grid which is assumed to be moving with respect to the flow and its velocity components are equal to those of the rotor. This makes it possible to simulate the flow through the rotor without any need of deformation in the grid.
Consideringthe finite volume approach, the governing equations will be of the following form:

$$V\frac{\partial Q}{\partial t}+\int\overrightarrow{Flux}.\overrightarrow{ds}=0 \quad (4)$$

Where

$$\overrightarrow{Flux}=(Fi+Gj)\overrightarrow{ds}=\left(n_xi+n_yj\right)ds \quad (5)$$

The flux terms are calculated using Roe's method [1] for its consideration of information propagation direction and high resolution of shock waves.[4] Fluxes through cell faces are evaluated considering a so called couple of "left" and "right" states and an artificial viscosity term to eliminate the spatial fluctuations near the shocks:

$$\overrightarrow{Flux}.\vec{n}=\frac{1}{2}\left[Flux(q_R)+Flux(q_L)-\widetilde{A}\,(q_R-q_L)\right] \quad (6)$$

Here, q is the primitive variables vector, i.e. q = [ρ u v p]^T. The term $\widetilde{A}\,(q_L-q_R)$ is calculated using Roe's method generalization proposed by Liu et al. [2, 5-7] and has a form of:

$$\widetilde{A}\,(q_R-q_L)=\left|\widetilde{\lambda_1}\right|\Delta Q+\delta_1\tilde{q}^{\,*}+\ \delta_2\,N_n \quad (7)$$

Where

$$\delta_1=\left(-\left|\widetilde{\lambda_1}\right|+\frac{\left|\widetilde{\lambda_2}\right|+\left|\widetilde{\lambda_3}\right|}{2}\right)\frac{\Delta p}{\tilde{c}^{\,2}}+\frac{\left|\widetilde{\lambda_2}\right|-\left|\widetilde{\lambda_3}\right|}{2}\frac{\tilde{\rho}\,\Delta U}{\tilde{c}} \quad (8)$$

$$\delta_2=\left(-\left|\widetilde{\lambda_1}\right|+\frac{\left|\widetilde{\lambda_2}\right|+\left|\widetilde{\lambda_3}\right|}{2}\right)\tilde{\rho}\,\Delta U+\frac{\left|\widetilde{\lambda_2}\right|-\left|\widetilde{\lambda_3}\right|}{2}\frac{\Delta p}{\tilde{c}} \quad (9)$$

$$\tilde{q}^{\,*}=\begin{bmatrix}1\\ \tilde{u}\\ \tilde{v}\\ \tilde{H}_o\end{bmatrix}N_n=\begin{bmatrix}0\\ n_x\\ n_y\\ \tilde{V}\end{bmatrix} \quad (10)$$

$\lambda_1$toλ_3 represent the three distinct eigenvalues of the jacobian matrix A:

$$\lambda_1 = U \ , \qquad \lambda_2 = U + c \ , \quad \lambda_3 = U - c \tag{11}$$

U is the normal to face component of the fluid relative velocity with respect to the face and the "~" symbol indicates Roe average values defined as following:

$$\tilde{\rho} = \sqrt{\rho_L \rho_R} \tag{12}$$

$$\tilde{\varphi} = \frac{\sqrt{\rho_L}\varphi_L + \sqrt{\rho_R}\varphi_R}{\sqrt{\rho_L} + \sqrt{\rho_R}} \quad \varphi = u, v, H_o \tag{13}$$

And the delta terms indicate the difference between the right and left states.

In order to eliminate any unphysical expansion shock, a mixed entropy correction is employed that changes all the eigenvalues of the Roe's method on proper conditions as proposed by Phogtanapanich et al.: [3]

$$|\lambda| = \begin{cases} |\lambda| & \lambda = U \pm c \ , \ |\lambda| \geq 2\eta^{VL} \\ \dfrac{|\lambda|^2}{4\eta^{VL}} + \eta^{VL} & \lambda = U \pm c \ , \ |\lambda| < 2\eta^{VL} \\ max(|\lambda|, \eta^{PA}) & \lambda = U \end{cases} \tag{14}$$

The parameter η^{VL} according to Van Leer et al. [8] is defined as:

$$\eta^{VL} = max(\lambda_R - \lambda_L, 0) \tag{15}$$

$$\lambda_R = U_R \pm c_R \lambda_L = U_L \pm c_L \tag{16}$$

And η^{PA} corresponds to a two dimensional entropy fix called the "H correction" proposed by Pandolfi et al. [9]. It involves four adjacent faces around the face for which fluxes are being calculated:

$$\eta^{PA} = max(\eta_1, \eta_2, \eta_3, \eta_4) \tag{17}$$

$$\eta_i = \frac{1}{2}|\lambda_R - \lambda_L|_i \tag{18}$$

Where η_1 to η_4 belong to the faces shown in figure 1.

BOUNDARY CONDITIONS

In general, the type of the boundary conditions on each boundary is determined by the characteristics along which the information propagates from or into the computational domain.

At inlet, the values of total pressure and total temperature and the direction of flow are usually known from the experimental data. The fourth condition is established by solving the one dimensional Riemann characteristic equation:

$$\frac{\partial}{\partial s}\left(\frac{2c}{\gamma - 1} - V_n\right) = 0 \tag{19}$$

or,

$$\left[\frac{2c}{\gamma - 1} - u\right]_{inlet} = \left[\frac{2c}{\gamma - 1} - u\right]_{interior} \tag{20}$$

At the outlet boundary, static pressure value is fixed and all other flow variables are extrapolated from the interior of the domain.

On the blades, solid wall conditions appropriate for inviscid flow are applied. Impermeability of the wall implies that the normal component of the fluid velocity must be equal to the normal to blade component of the velocity of the rotor. On the other hand, the absence of viscosity effects will result in the slipping of the flow along the blade and so, the tangential component of fluid velocity is calculated through an extrapolation. Two extra boundary conditions are gained by extrapolating the density and the static pressure from the interior of the domain..

VALIDATION STUDIES

The numerical method has been validated against a number of available test cases. First one is the Sod shock tube problem which is a known analytical test case for evaluation of numerical schemes used for the simulation of compressible flows. Two cases of this problem based on the values chosen by Hirsch [10] have been studied. The results of numerical simulations and exact solutions are compared in figures 2 and 3 where they show good agreements.

Second case is inviscid flow inside a converging-diverging nozzle for which analytical solution predicts a shock wave inside the diverging part. Here again, satisfactory results are obtained using the method of the present study. Figures 4 to 7 demonstrate the numerical solution obtained. A comparison of some parameters calculated from the numerical results and the analytical solution is presented in table 1.

A third test case including flow inside a channel has been studied for which geometry consists of a circular bump with a 10 percent of chord maximum thickness on the middle of the channel. Two cases of this problem with different inlet mach numbers are subject to test in this study. The first one corresponds to a subsonic flow with inlet mach number of M=0.5 where a symmetric distribution of mach number is predicted by the numerical simulation. In the second case, an inlet mach number of M=0.675 results in a transonic flow for which a shock wave is predicted over the bump. Results of the present numerical method are compared with the results of two other methods studied by Eraslan [11] in Figures 8 and 9.

RESULTS

The simulation of axial compressor rotor flow has been carried out for the midspan section of a transonic rotor called NASA Rotor 35. This rotor has a rotational speed of 16043 rpm and a design pressure ratio equal to 1.63. A schematic of the computational grid used for this rotor can be seen in figure 10. Design and off-design conditions have been studied for Rotor 35 where rotor speed varies from 60 to 100 percent of the design value. Inlet conditions are the same for all speeds but the back pressure values differ according to the experimental data.

A shock wave is predicted near the trailing edge at rotor speeds between 70 and 100 percent of design value by solving the system of Euler equations. The static pressure is observed to drop entering the flow passage and then rise up to the back pressure value at all studied speeds. A high pressure region forms at the leading edge of the rotor that tends to taper as the rotor speed increases. (Figures 11 to 14)

As the rotor does work on the fluid passing through, energy level of the fluid rises. The increase in total pressure and total temperature of the flow obtained from the numerical results and the experimental data of Reid et al. [12, 13] are compared in figures 15 and 16.

Table 1. Comparison of results for converging-diverging nozzle

	Analytical Solution	Present Study
Mach Number Before Shock	1.6	1.59
Exit Mach Number	0.5	0.51
Total Pressure after shock (kPa)	177.9	178.6
shock location (m)*	0.07	0.073

* Nozzle area is a function of x-coordinate

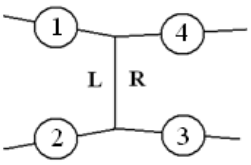

Figure 1. Faces involved in H correction

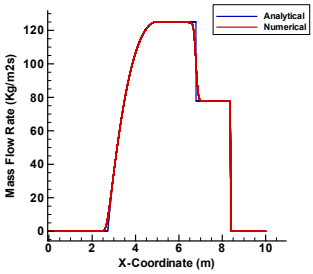

Figure 2. Comparison of numerical and analytical solutions for the shock tube problem - First case

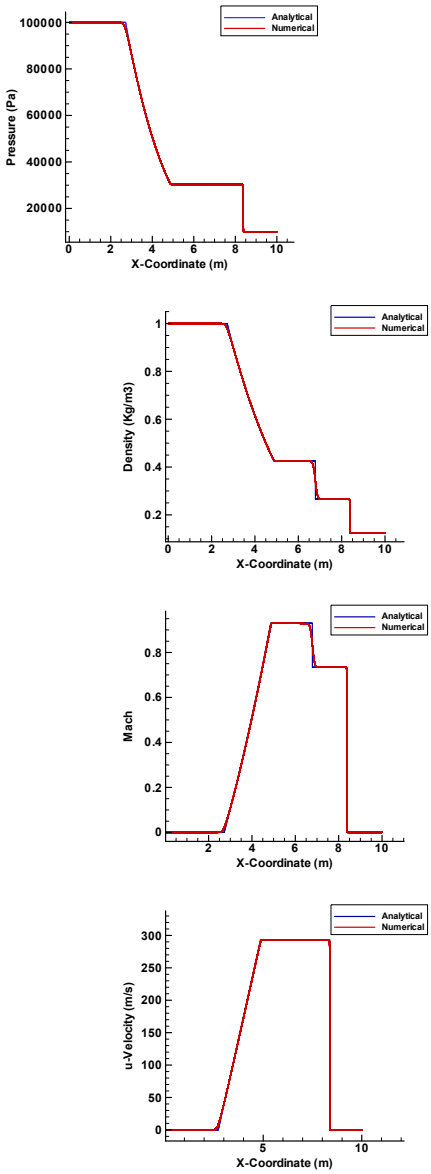

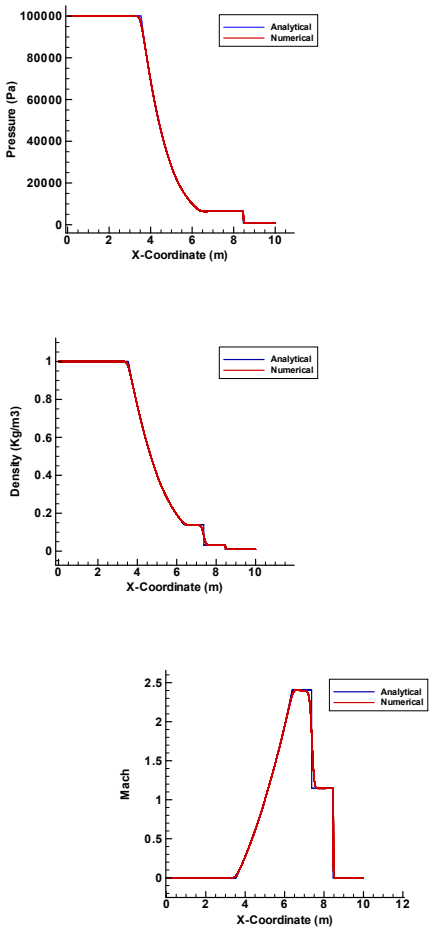

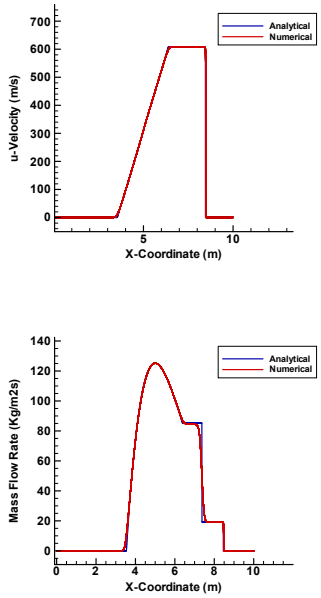

Figure 3. Comparison of numerical and analytical solutions for the shock tube problem - Second case

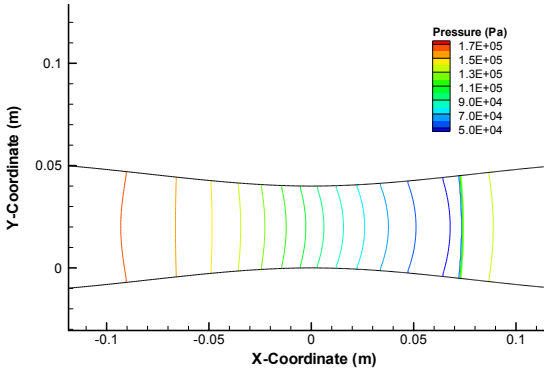

Figure 4. Static pressure contours in converging-diverging nozzle

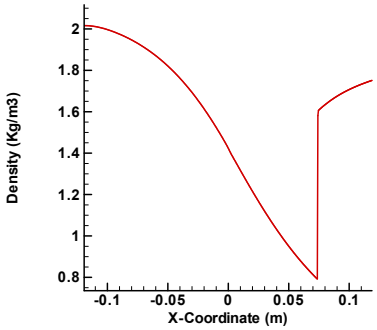

Figure 5. Density distribution along the centerline of converging-diverging nozzle

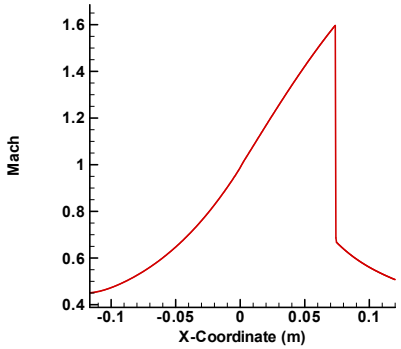

Figure 6. Mach number distribution along the centerline of converging-diverging nozzle

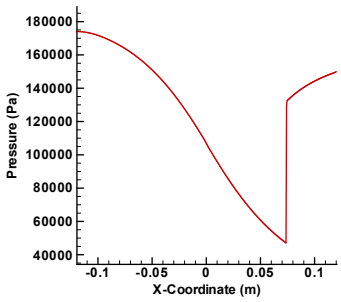

Figure 7. Static pressure distribution along the centerline of converging-diverging nozzle

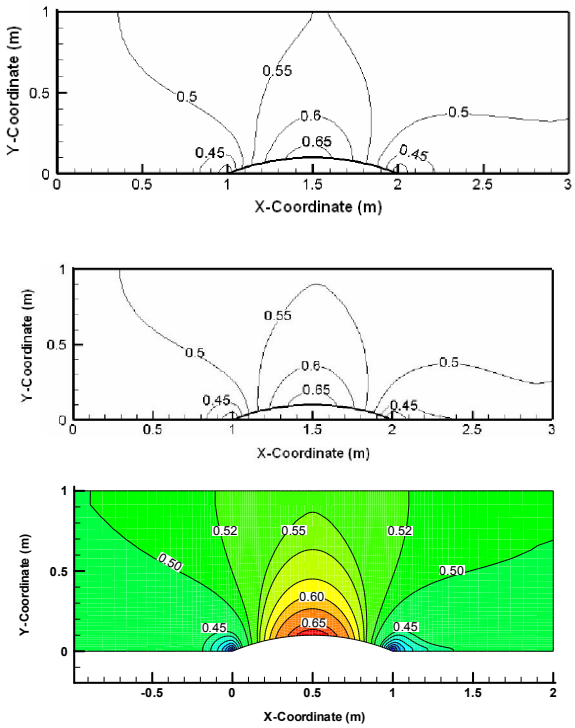

Figure 8. Comparison of mach number in the bump in a channel test case using Van Leer FVS (up), AUSM (middle) and the method of present study (down) for M=0.5

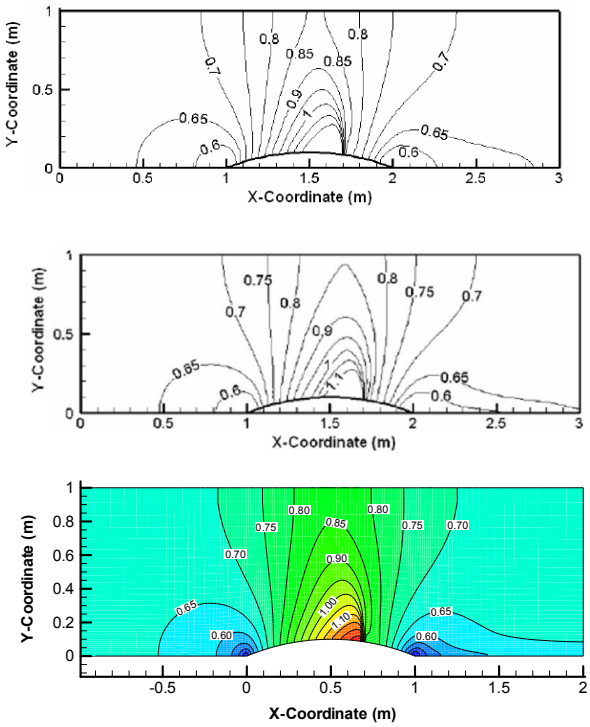

Figure 9. Comparison of mach number contours in the bump in a channel test case using Van Leer FVS (up), AUSM (middle) and the method of present study (down) for M=0.675

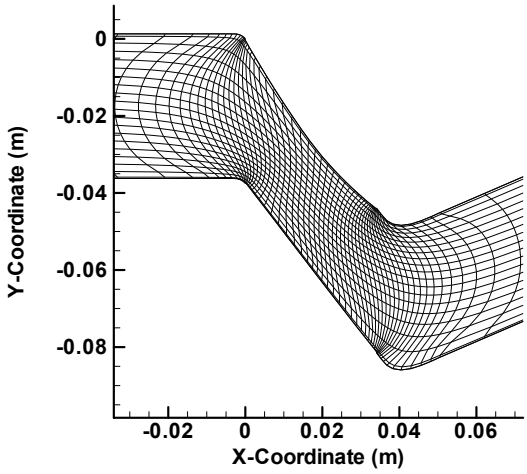

Figure 10. Computational grid for Rotor 35. (One out of every 25 nodes is shown)

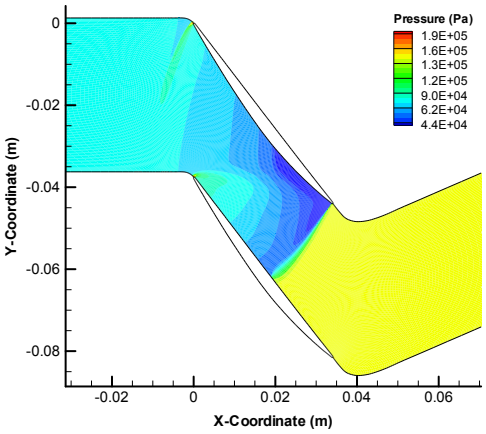

Figure 11. Static pressure contours at 100% design speed

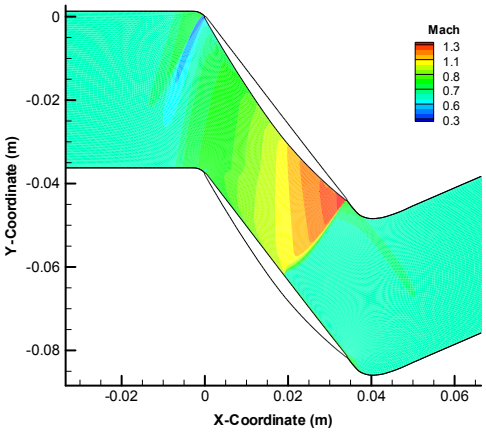

Figure 12. Mach number contours at 100% design speed

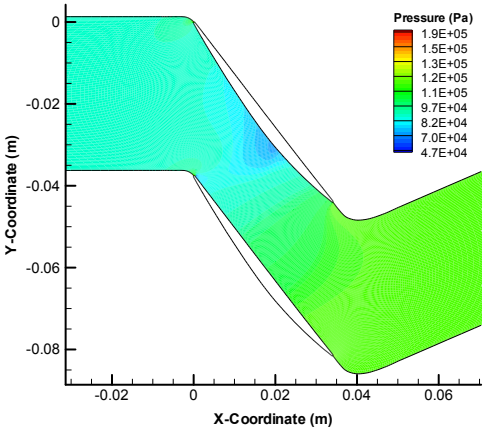

Figure 13. Static pressure contours at 60% design speed